

Spectroscopic and Semiempirical Studies of a Proton Channel Formed by the Methyl Ester of Monensin A

Adam Huczyński,[†] Piotr Przybylski,[†] Bogumil Brzezinski,^{*,†} and Franz Bartl[‡]

Faculty of Chemistry, A. Mickiewicz University, Grunwaldzka 6, 60-780 Poznan, Poland, and Institute of Medical Physics and Biophysics, Charité Universitätsmedizin Berlin, Campus Charité Mitte, Ziegelstrasse 5/9, 10117 Berlin, Germany

Received: April 6, 2006; In Final Form: May 29, 2006

Monensin A is an ionophore able to carry protons and cations through the cell membrane. Its methyl ester (MON1) and its hydrates have been studied in acetonitrile, and its deuterated analogue by Fourier transform infrared (FTIR) and ¹H and ¹³C NMR spectroscopies as well as by vapor pressure osmotic and PM5 semiempirical methods. Interestingly, these hydrates show new and unexpected biophysical and biochemical properties. The formation of the hydrates starts with a transfer of a proton from the O_{IV}–H hydroxyl group of MON1 to an oxygen atom of a water molecule, which is subsequently hydrated by other water molecules forming the (MON1 + 3H₂O) species. This hydrate exhibits a ringlike structure in which the water molecules form an almost linear hydrogen-bonded chain. Within this chain, the excess proton fluctuates very fast inside the water cluster as indicated by a continuous absorption in the FTIR spectra. The formation of the (MON1 + 3H₂O) species is accompanied by a self-assembly process, leading to the formation of a proton channel made up of eight (MON1 + 3H₂O) units with a length of 60 Å, in which the proton can fluctuate over the whole distance. Semiempirical calculations suggest that due to the hydrophobic surface the channel can be incorporated readily in a lipid bilayer. This hypothetical new channel is thought to be able to transport protons through the cell membrane. Thus it is a suitable model for studying proton-transfer processes, and in addition, it may open interesting new fields of application.

Introduction

Monensin A (Chart 1) is a carboxylic polyether ionophore isolated from *Streptomyces cinnamomensis*.^{1,2} Due to its lipophilic surface and its polar inner core containing six ether oxygen atoms, three hydroxyl groups, and one carboxylic group, monensin is well-suited for transporting monovalent cations, especially H⁺, Na⁺, and K⁺, across lipid membranes.^{3–20} These properties have stimulated a multiplicity of possible biological and pharmaceutical applications of this compound. It exhibits antibiotic,^{21–26} coccidiostatic,^{27–29} cardiovascular,³⁰ and other important biological and medical properties.^{31–43} Up to now various modifications of monensin have been synthesized to obtain less toxic derivatives,^{44–52} enabling expansion of its fields of application.

Monensin A methyl ester was previously synthesized either by treating monensin with methyl iodide and 1,8-diazabicyclo-[5.4.0]undec-7-ene (DBU)⁵³ or by treating monensin sodium salt with methyl bromide and cryptand [2.2.2].⁴⁹

In the present study, we synthesized the monensin methyl ester by our method, described previously.⁵⁴ This ester is able to form hydrates with water molecules, which has never been observed before. The properties of these hydrates were investigated by Fourier transform infrared (FTIR) and ¹H and ¹³C NMR spectroscopies as well as by a vapor pressure osmotic (VPO) method and the PM5 semiempirical method.

Experimental Methods

The monensin A sodium salt was purchased from Sigma (90–95%). CD₃CN and CH₃CN spectral-grade solvents were stored over 3 Å molecular sieves for several days.

Synthesis of the Monensin A Methyl Ester. Monensinic acid (MON A) was obtained by stirring a dichloromethane solution of monensin A sodium salt vigorously with a layer of aqueous sulfuric acid. The organic layer containing MON A was washed with distilled water until the washings were neutral and then evaporated under reduced pressure to dryness.

Monensin A methyl ester (MON1) was then obtained by following our method given in ref 54.

Preparation of the Mixtures of MON1 with Water. The mixtures were prepared in a 1 mL standard flask. Approximately 0.5 mL of 0.14 M acetonitrile solution of MON1 was placed in the flask, and a respective amount of a standard solution of water was added. The flask was filled with acetonitrile to obtain exactly 1 mL of volume. The standard solution was prepared by dissolving 630 mg of water in absolute acetonitrile in a 5 mL standard flask. From this solution 20, 30, and 70 μL were used to obtain 1:2, 1:3, 1:7, etc. ratios of MON1 to water, respectively. For the NMR measurements, instead of CH₃CN, CD₃CN was used. All manipulations of the samples were performed under argon atmosphere.

Spectroscopic Measurements. The FTIR spectra of monensin A methyl ester and its hydrates were recorded in the mid-infrared region in 0.07 mol L^{−1} acetonitrile solutions.

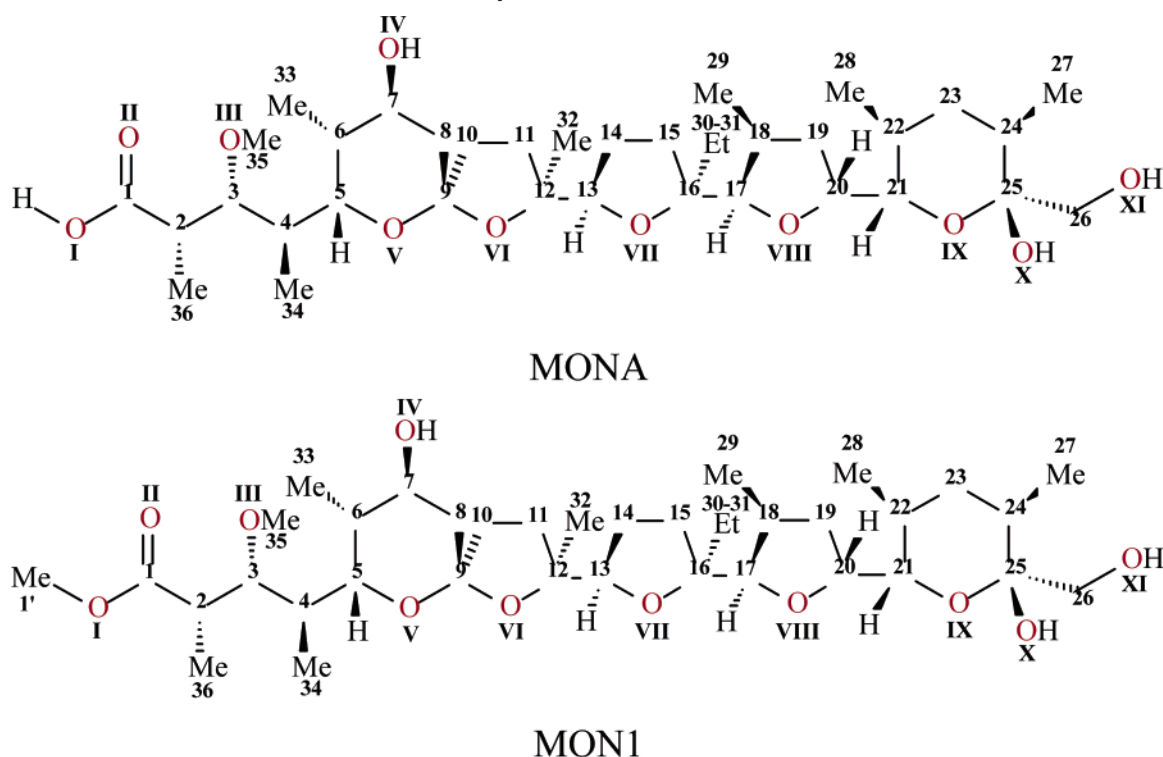
A cell with Si windows and wedge-shaped layers was used to avoid interferences (mean layer thickness 170 μm). The spectra were taken with an IFS 113v FTIR spectrophotometer

* Author to whom correspondence should be addressed. Phone: +48-61-8291330. E-mail: bbrzez@main.amu.edu.pl.

[†] A. Mickiewicz University.

[‡] Charité Universitätsmedizin Berlin.

CHART 1: Structures of Monensin A and Its Methyl Ester



(Bruker, Karlsruhe) equipped with a deuterated triglycine sulfate (DTGS) detector: resolution, 2 cm^{-1} ; number of scans (NSS) = 125. The Happ–Genzel apodization function was used.

All manipulations of the substances were performed in a carefully dried and CO_2 -free glovebox.

The NMR spectra of monensin A methyl ester and its hydrate were recorded in 0.07 mol L^{-1} CD_3CN solutions using a Varian Gemini 300 MHz spectrometer. All spectra were locked to the deuterium resonance of CD_3CN .

The ^1H NMR measurements in CD_3CN were carried out at the operating frequency 300.075 MHz: flip angle, $\text{pw} = 45^\circ$; spectral width, $\text{sw} = 4500\text{ Hz}$; acquisition time, $\text{at} = 2.0\text{ s}$; relaxation delay, $d_1 = 1.0\text{ s}$; $T = 293.0\text{ K}$ and using trimethylsilane (TMS) as the internal standard. No window function or zero filling was used. Digital resolution is 0.2 Hz per point . The error of the chemical shift value was 0.01 ppm .

^{13}C NMR spectra were recorded at the operating frequency 75.454 MHz : $\text{pw} = 60^\circ$; $\text{sw} = 19\,000\text{ Hz}$; $\text{at} = 1.8\text{ s}$; $d_1 = 1.0\text{ s}$; $T = 293.0\text{ K}$ and TMS as the internal standard. Line broadening parameters were 0.5 or 1 Hz . The error of the chemical shift value was 0.01 ppm .

The ^1H and ^{13}C NMR signals were assigned for each species using one- or two-dimensional (COSY, HETCOR, NOESY, GHMBC, and GHSQC) spectra.

Vapor Pressure Osmometric Measurements. Vapor pressure osmometric measurements of acetonitrile solutions were recorded on the Knauer pressure osmometer using probes for nonaqueous solutions. Two concentrations (0.05 and 0.10 mol L^{-1}) of MON1 with and without the addition of water in acetonitrile solutions were measured. Acetonitrile with the respective quantity of water was used as a reference.

PM5 Calculations. PM5 semiempirical calculations were performed in the gas phase and in the lipid bilayer using the WinMopac 2003 program.^{55,56} In all cases, a full geometry optimization of monensin A methyl ester and its hydrates was carried out without any symmetry constraints.⁵⁷

Results and Discussions

The structure of the monensin A and its methyl ester together with the atom numbering is shown in Chart 1.

^1H and ^{13}C NMR Measurements. The ^1H and ^{13}C NMR data of MON1 in acetonitrile and its 1:3 mixture with water molecules are compared in Table 1. We only show the NMR data of this monensin/water ratio because the positions of the ^1H and ^{13}C signals do not change significantly with higher monensin/water ratios. This demonstrates that the addition of three water molecules to the solution of MON1 is sufficient to induce the structural changes described in the following, which can then be monitored by NMR spectroscopy.

In the spectrum of water-free MON1, the $\text{O}_{\text{IV}}\text{--H}$ proton signal arises as a doublet at 4.15 ppm , the $\text{O}_{\text{XI}}\text{--H}$ proton as a triplet at 2.86 ppm , and the $\text{O}_{\text{X}}\text{--H}$ proton as a singlet at 3.90 ppm . After the addition of water molecules, the $\text{O}_{\text{IV}}\text{--H}$ proton signal is no longer observed, and the other two signals of $\text{O}_{\text{XI}}\text{--H}$ and $\text{O}_{\text{X}}\text{--H}$ protons become broadened and shifted toward 2.92 and 3.39 ppm , respectively. The chemical shift of the $\text{O}_{\text{X}}\text{--H}$ proton indicates that after the addition of water molecules, this group is involved in a slightly weaker hydrogen bond than in the MON1 molecule. It is interesting to note that neither the proton from the $\text{O}_{\text{IV}}\text{--H}$ group nor the two protons of the water molecule added are observed in the spectrum. This is the first hint that the proton that localized to the $\text{O}_{\text{IV}}\text{--H}$ group before the addition of water is not located at a specific water molecule but is delocalized in the water cluster within the inner core of MON1. This means that these protons undergo a dynamic change. The delocalization of $\text{O}_{\text{IV}}\text{--H}$, especially the ionization of this group, is confirmed by the loss of the couplings of the $\text{O}_{\text{IV}}\text{--H}$ proton with the C_6 , C_7 , and C_8 carbon atoms in the GHMBC experiment. The signals of all other protons remain in unchanged positions upon the addition of water, and the signals of the respective $\text{C}\text{--H}$ protons, coupled with the OH protons, become less complex. The addition of water has a significant effect on the ^{13}C NMR spectrum of MON1,

TABLE 1: ^1H and ^{13}C NMR Chemical Shifts (ppm) of Proton and Carbon Atom Signals of MON1 and Its Complex with 3 H_2O Molecules^a

atom no.	^1H NMR shifts (ppm)			^{13}C NMR shifts (ppm)		
	MON1	MON1 + $3\text{H}_2\text{O}$	Δ	MON1	MON1 + $3\text{H}_2\text{O}$	Δ
1				176.46	176.40	0.06
2	2.63 dq	2.64 dq	-0.01	41.47	41.31	0.16
3	3.51 t	3.52 t	-0.01	82.37	82.24	0.13
4	1.99	1.94	0.05	37.78	37.60	0.18
5	3.96 dd	3.96 dd	0.00	68.48	68.35	0.13
6	1.72	1.73	-0.01	36.92	36.78	0.14
7	3.67	3.70	-0.03	71.91	71.65	0.26
8A	1.65	1.56	0.09	35.06	34.85	0.21
8B	1.99	1.94	0.05			
9				108.49	108.34	0.15
10A	1.87	1.85	0.02	39.74	39.58	0.16
10B	1.92	1.92	0.00			
11A	1.74	1.62	0.12	32.68	32.58	0.10
11B	1.98	2.04	-0.06			
12				87.00	86.84	0.16
13	3.64 dd	3.67	-0.03	84.44	84.12	0.32
14A	1.59	1.50	0.09	28.44	28.18	0.26
14B	1.77	1.77	0.00			
15A	1.59	1.59	0.00	32.05	31.81	0.24
15B	2.10	2.01	0.09			
16				88.03	87.77	0.26
17	3.87 d	3.88 d	-0.01	86.37	86.11	0.26
18	2.24	2.20	0.04	35.91	35.67	0.24
19A	1.49	1.51	-0.02	34.63	34.36	0.27
19B	2.14	2.15	-0.01			
20	4.22 ddd	4.22 ddd	0.00	78.03	77.84	0.19
21	3.60 dd	3.66	-0.06	77.25	76.96	0.29
22	1.31	1.41	-0.10	34.04	33.73	0.31
23A	1.25	1.30	-0.05	37.65	37.42	0.23
23B	1.43	1.44	-0.01			
24	1.68	1.67	0.01	34.77	34.68	0.09
25				97.97	97.89	0.08
26	3.34 dd	3.36 s	-0.02	67.36	67.17	0.19
27	0.82 d	0.82 d	0.00	16.46	16.26	0.20
28	0.86 d	0.86 d	0.00	17.82	17.56	0.26
29	0.95 d	0.95 d	0.00	16.11	15.88	0.23
30	1.56	1.55	0.01	30.11	29.91	0.20
31	0.89 t	0.89 t	0.00	8.29	8.08	0.21
32	1.34 s	1.35 s	-0.01	26.29	26.19	0.10
33	0.89 d	0.89 d	0.00	11.30	11.08	0.22
34	0.97 d	0.97 d	0.00	12.40	12.26	0.14
35	3.29 s	3.29 s	0.00	58.48	58.33	0.15
36	1.13 d	1.14 d	-0.01	12.66	12.38	0.28
1'	3.66 s	3.65 s	0.01	52.35	52.17	0.18
O _{XI} H	2.86 t	2.92 vbr	-0.07			
O _{IV} H	4.15 d					
O _X H	3.90 s	3.39 br	0.51			

^a MON1 + $3\text{H}_2\text{O}$ = 1:3 molar ratio of MON1 to water; Δ = $\delta_{\text{MON1}} - \delta_{\text{MON1}+3\text{H}_2\text{O}}$.

manifested as a shift of the signals of all carbon atoms toward lower ppm values. The greatest shifts are observed for the carbon atoms bonded with the oxygen atoms involved in the hydrogen bonds with water molecules as well as for the C_7 carbon atom. It would be expected that the ionization of the $\text{O}_{\text{IV}}\text{-H}$ group should be better reflected in the ^{13}C NMR spectra, especially for the chemical shift of the C_7 carbon. The observed $\Delta = 0.26$ ppm value for the C_7 atom suggests a presence of a relatively strong $\text{O}_{\text{IV}}\text{-}\cdots\text{H-O}^+\text{H}_2$ hydrogen bond, which decreases this ionization effect. The ^{13}C NMR data taken together suggest that the binding of the water molecules can be realized only in a ringlike structure of the MON1 molecule. This suggestion is confirmed by the NOESY spectra results of the 1:3 mixture of MON1 with water molecules in CD_3CN . In this two-dimensional experiment, we found the existence of the coupling between the $\text{O}_\text{X}\text{-H}$ proton and the protons of the O-CH_3 ester group

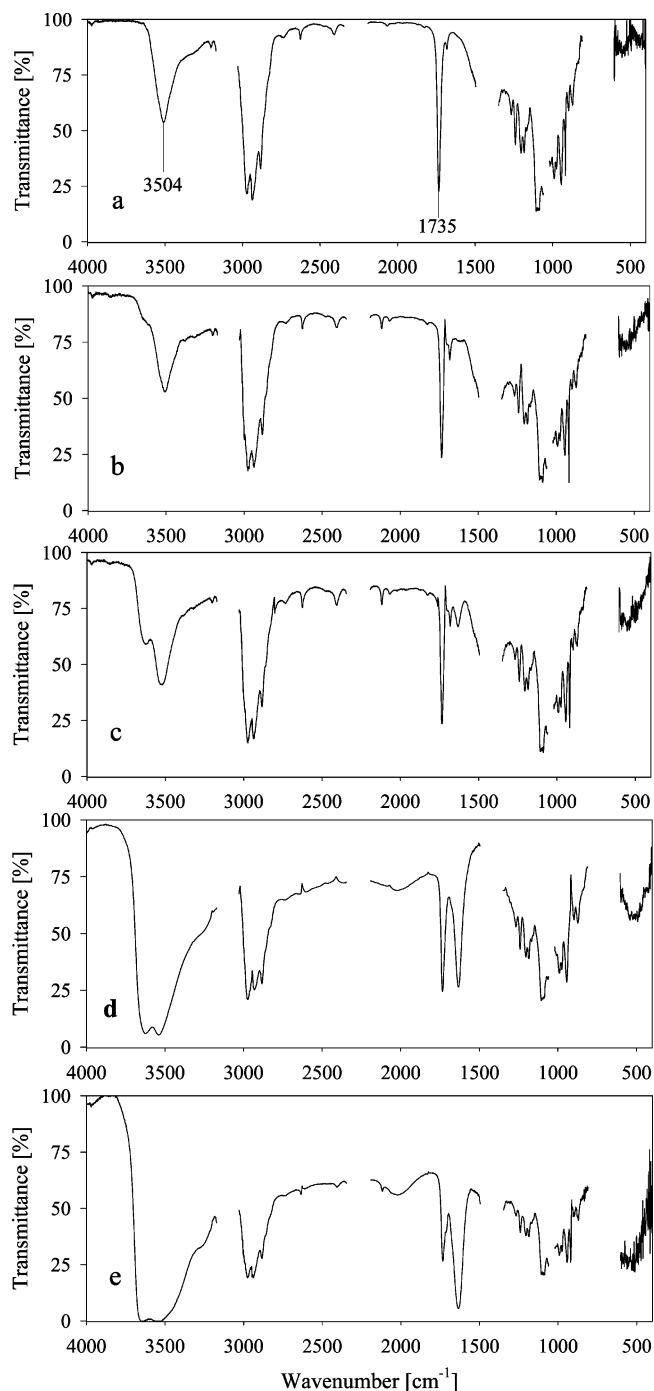


Figure 1. FTIR spectra of the acetonitrile solutions of (a) MON1, (b) 1:2 mixture of MON1 with water molecules, (c) 1:3 mixture of MON1 with water molecules, (d) 1:7 mixture of MON1 with water molecules, and (e) 1:12 mixture of MON1 with water molecules.

as well as the couplings of the $\text{O}_{\text{XI}}\text{-H}$ proton with $\text{C}_2\text{-H}$ and OMe_{35} protons.

Fourier Transform Infrared Studies. The FTIR spectra of water-free MON1 as well as its mixture with water molecules of various ratios are shown in Figures 1a–e. To discriminate between water molecules involved in hydrate formation and those assigned to the solvent, the spectrum of 0.42 mol L^{-1} water in acetonitrile is given in Figure 2. The latter spectrum shows the typical bands assigned to the $\nu_{\text{as}}(\text{OH})$ and $\nu_{\text{s}}(\text{OH})$ stretching vibrations at 3637 and 3545 cm^{-1} , respectively, and the deformation $\delta(\text{OH})$ and $\gamma(\text{OH})$ bending vibrations at 1635 and 1500 cm^{-1} , respectively. Additionally, the band of a very weak combination $[\delta(\text{OH}) + \gamma(\text{OH})]$ vibration at 2026 cm^{-1} is

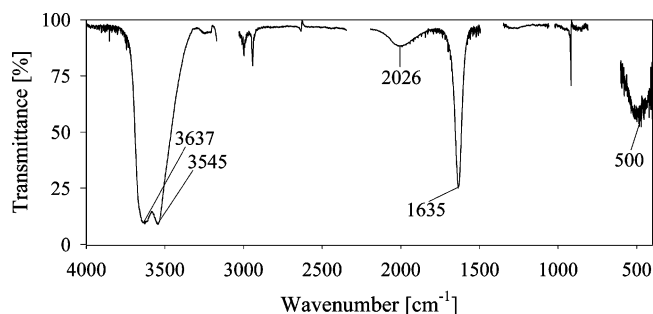
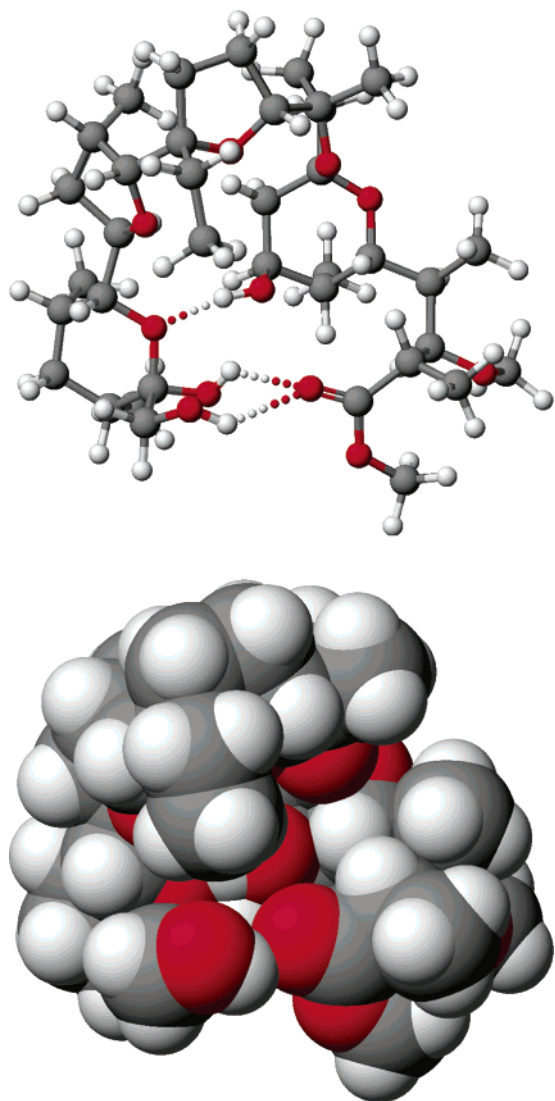


Figure 2. FTIR spectrum of water in the acetonitrile solution, concentration 0.42 mol L^{-1} .

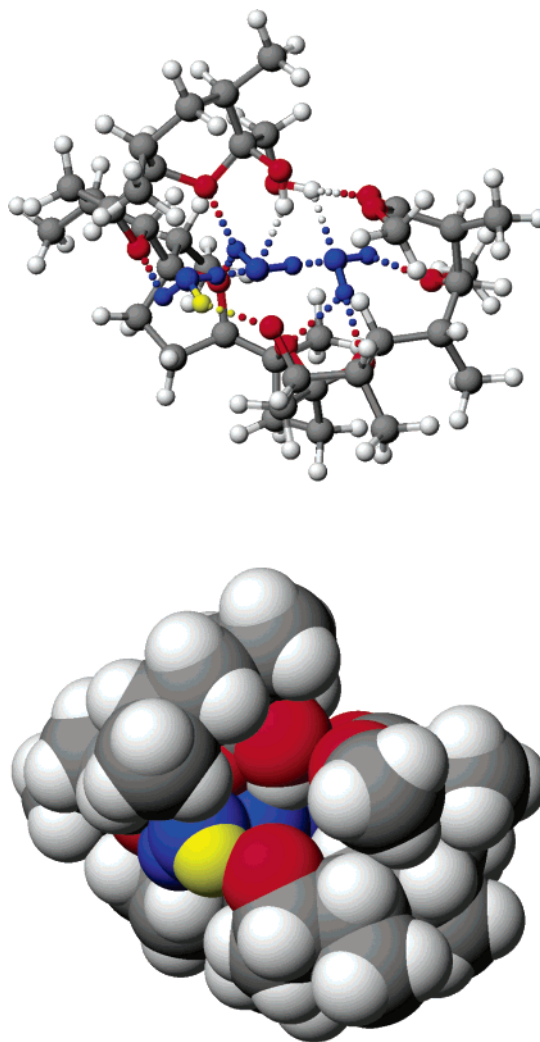
CHART 2: Ball and Stick Projection of the MON1 Structure Calculated in the Gas Phase by the PM5 Method



also observed.^{58,59} The analytical band of $\delta(\text{OH})$ bending vibrations at 1635 cm^{-1} that contains the information on the number of water molecules bonded to acetonitrile molecules and not to MON1 has been chosen because it is not superimposed by any bands of MON1.

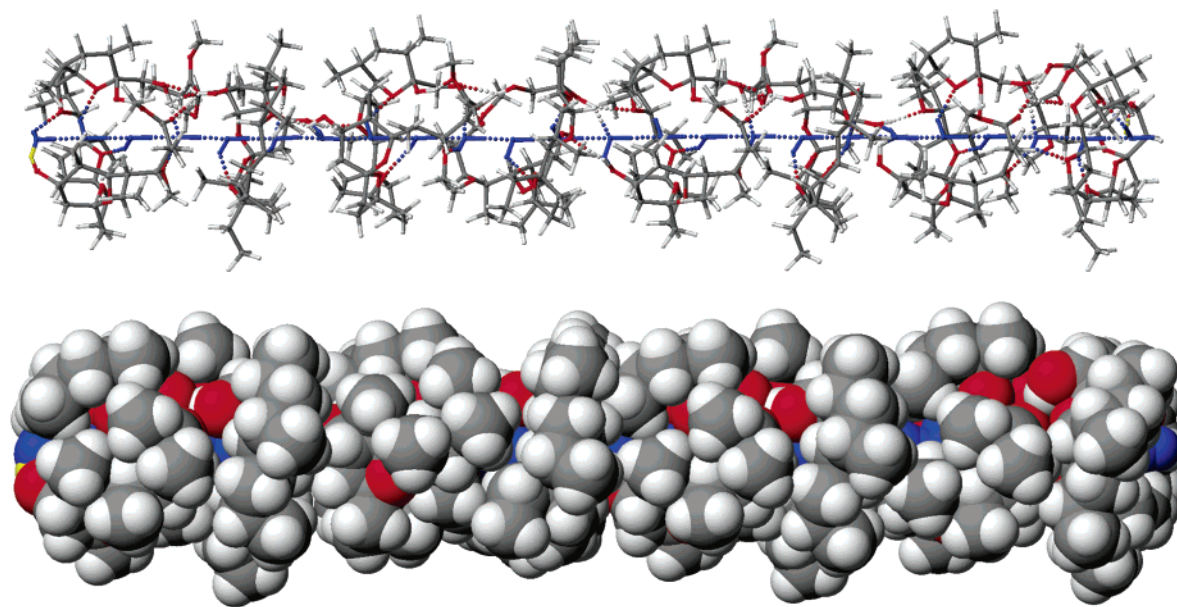
Surprisingly, in the spectrum of MON1/water at a ratio of 1:2 (Figure 1b), a continuous absorption beginning at about 3700 cm^{-1} and extending over the whole region is found. Such a continuous absorption in the IR spectra indicates the fast fluctuation of an excess proton within the so-called Zundel's

CHART 3: Ball and Stick Projection of the MON1 + $3\text{H}_2\text{O}$ Hydrate Structure Calculated in the Gas Phase by the PM5 Method



cation (H_5O_2^+).^{60,61} The formation of this group is only possible if the proton, which was, according to the NMR data, released from the $\text{O}_{\text{IV}}\text{--H}$ hydroxyl group of MON1, becomes incorporated between two water molecules where it fluctuates on a picosecond time scale. The H_5O_2^+ cation is an important group because of the high mobility of the proton along the homoconjugated $\text{OH}\cdots\text{H}$ hydrogen bond that connects the two water molecules and enables the transport of a proton from one water molecule to the other. The fast fluctuation of the proton is also the reason the spectrum of the 1:2 complex shows almost no bands of free water molecules bonded to the acetonitrile molecules. This interpretation is consistent with the ^1H NMR data discussed above, according to which no proton signals of free water could be detected, as well as with the results of the PM5 semiempirical calculation as discussed above.

In the spectrum of the 1:3 MON1/water mixture (Figure 1c), the intensity of the continuous absorption only slightly increases. This observation suggests that with an increasing concentration of water, a third water molecule is incorporated, forming a $\text{MON1}^- \text{anion--H}_7\text{O}_3^+$ species. As in the H_5O_2^+ species, the water molecules form an almost linear hydrogen-bonded chain within the ringlike structure of MON1 (Chart 3), in which the proton can fluctuate in a chain elongated by one water molecule, causing a slight increase in the continuous absorption. Such an interpretation is in agreement with previous theoretical studies.⁶²

CHART 4: Ball and Stick Projection of the Proton Channel Structure Made Up of Eight (MON1 + 3H₂O) Species Calculated in the Gas Phase by the PM5 Method

This process is, however, not quantitative as shown by a visible increase in the intensity of characteristic bands of water molecules at 3637 and 3545 cm^{-1} as well as at 1635 cm^{-1} observed in acetonitrile. Apart from the formation of a H_7O_3^+ species in the inner core of the ringlike structure, the addition of a third water molecule does not affect the basic structure of MON1.

The situation changes dramatically when increasing the concentration of water molecules in the solution of MON1 (ratio 1:7, Figure 1d). Now the intensity of the continuous absorption increases significantly. We would like to point out that such a strong increase in the continuum intensity cannot be explained by the simple formation of a species with a higher stoichiometry than H_7O_3^+ within MON1. A fourth water molecule would not fit in the pseudo-ring structure of H_7O_3^+ and would instead destroy the hydrogen-bonded complex, thus reducing the intensity of the continuum.

A possible mechanism responsible for such a dramatic absorption change of the continuum might be the self-assembly process of several MON1^- anion- H_7O_3^+ cation species, eventually leading to the formation of a proton channel made up of water molecules surrounded by a hydrophobic monensin matrix. In this channel, the proton can fluctuate over a distance of about 60 Å (Chart 4), which explains the strong increase in the continuous absorption. The strong increase in the intensities of the water bands at 3637 and 3545 cm^{-1} and at 1635 cm^{-1} in Figure 1d also indicates the presence of water molecules bonded to the acetonitrile molecules.

With the addition of more water molecules, the intensity of the continuous absorption still increases up to a ratio of 1:12 MON1/water (Figure 1e) and remains unchanged at higher water concentrations (data not shown). This demonstrates that at the ratio 1:12 all MON1 molecules are saturated with water molecules and that the self-assembly process leading to the formation of the proton channel has reached its maximum.

Now the question arises whether monensin is able to form complexes with water and thus to form analogous proton channels. The spectra of MONA in the presence of various amounts of water are shown in Figures 3a–d. Even in the presence of a large amount of water, no continuum can be observed in the spectra. These results indicate that the mech-

anism of proton transport achieved by monensin and its ester is fundamentally different and will be discussed below.

The biological activity of monensin is based on its ability to act as a Na^+/H^+ antiporter, thus transporting monovalent cations and protons in opposite directions across cell membranes.⁶³ The transport of protons out of the cell leads to an intracellular alkalization and/or disruption of the Na^+/K^+ balance, inducing cell death of bacteria or apoptosis of various types of cancer cells such as HL60.⁶⁴ Despite close structural similarities between monensin and its methyl ester, our data indicate possible differences in the mechanisms of proton transport. The available information suggests that at physiological pH the carboxyl group of monensin is negatively charged and therefore fixed in the aqueous medium near the membrane surface. The rest of the molecule, which is much more lipophilic, is anchored in the membrane. The mechanism of the monensin-mediated transport of cations across the lipid bilayer was discussed extensively in a number of publications.^{3,65–66}

For the ester at physiological pH, no negatively charged carboxyl group is present, which fixes the molecule to the aqueous medium near the extracellular side to capture a proton in an initial step of the transport mechanism. As described in the Results section, monensin has no significant affinity to water in contrast to its methyl ester. The ester may, therefore, use water molecules on the extracellular surface to form those hydrates. As indicated by the spectroscopic data, these hydrates form a channel by a self-assembly process with a water file in its inner core able to conduct protons and possibly other cations. Due to its hydrophobic surface, the channel can be incorporated into a lipid bilayer, thus transporting protons through the cell membrane.

After esterification, the molecule is now converted from a proton carrier into a proton channel, which makes the proton transport independent of the diffusion through the cell membrane. The mechanism of the proton transport in this channel is different and is based on the high polarizability of the proton moving very fast along the hydrogen bonds forming a channel, as indicated by the continuous absorptions in the infrared spectra. Proton channels with high proton polarizability due to very fast collective fluctuations in which an initial proton is shifted in a hydrogen-bonded single water file are not uncommon and have

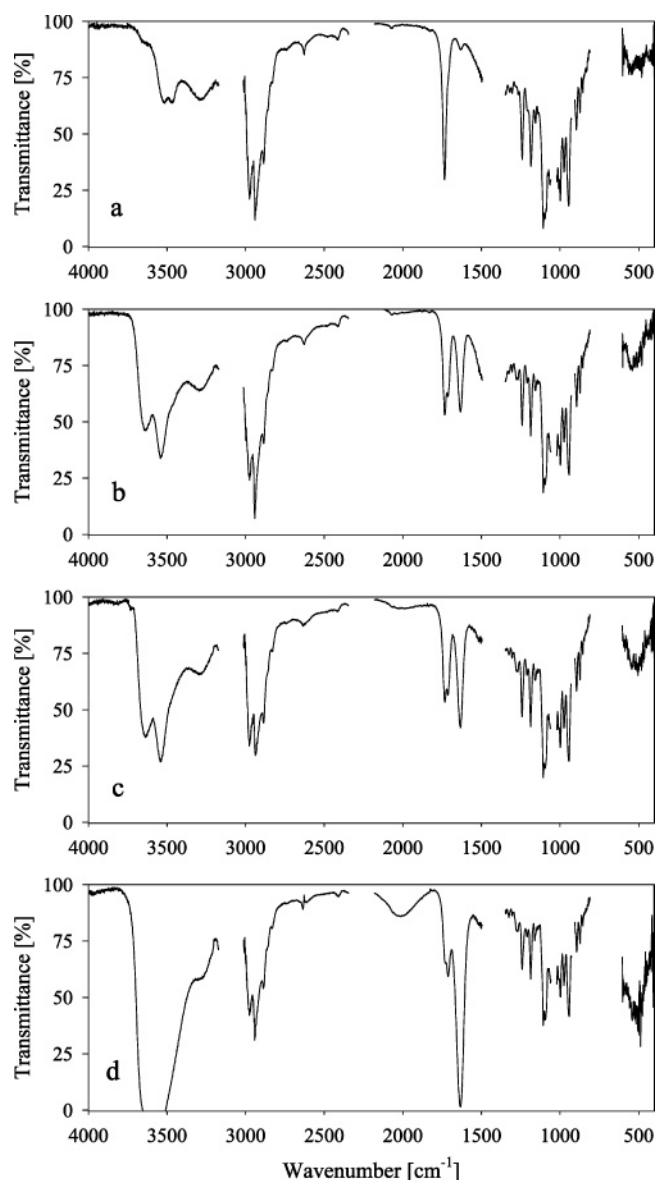


Figure 3. FTIR spectra of the acetonitrile solutions of (a) 1:2 mixture of MONA with water molecules, (b) 1:3 mixture of MONA with water molecules, (c) 1:7 mixture of MONA with water molecules, and (d) 1:12 mixture of MONA with water molecules.

been observed in other biological systems such as the cation- and proton-conducting channel in gramicidin (Bartl et al.⁶⁷). Another example is bacteriorhodopsin, located in the cell membrane of *Halobacterium salinarum*. Although not a proton channel like gramicidin, upon light absorption, it actively pumps protons across the membrane. A protonated water cluster is involved in the proton-transfer process (Garczarek et al.⁶⁸).

VPO Measurements. An independent technique to determine the molecular weight of organic molecules is to measure the osmotic pressure by using a vapor pressure osmometer. The osmometric data for water-free MON1 in acetonitrile solution and in the presence of water with stoichiometric ratios of MON1/water of 1:2, 1:3, 1:7, 1:12, and 1:20 are summarized in Table 2 and visualized in Figure 4. The osmotic coefficient value of ~ 1 for MON1 in acetonitrile solution suggests that the molecule exists as a monomer. The values do not change significantly for the mixtures of 1:2 and 1:3 stoichiometry with water, indicating that the stoichiometry of these hydrates is not influenced and the hydrates still exist as monomers. For the 1:7 stoichiometry, however, the osmotic coefficient decreases

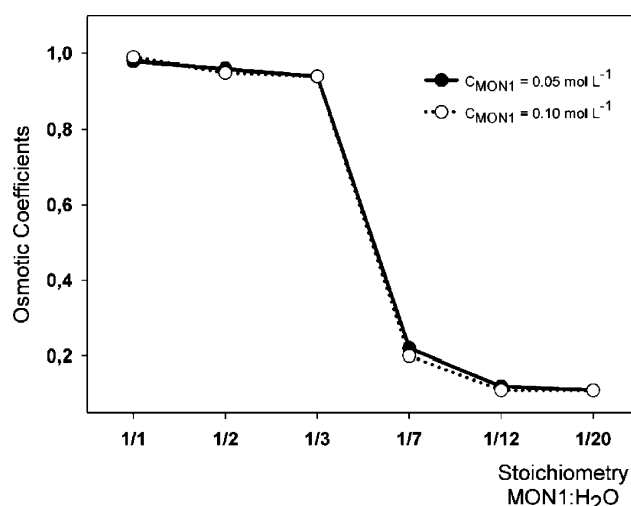


Figure 4. Osmotic coefficient versus stoichiometry of the MON1/H₂O mixture for the MON1 concentrations of (a) 0.05 and (b) 0.1 mol L⁻¹.

TABLE 2: Osmotic Coefficients of the Mixtures of MON1 with Various Quantities of Water in Acetonitrile Solution

mixture	stoichiometry MON1/water	concentration of MON1 (mol L ⁻¹)	
		0.05	0.10
MON1	1:0	0.98	0.99
MON1 + H ₂ O	1:2	0.96	0.95
MON1 + H ₂ O	1:3	0.94	0.94
MON1 + H ₂ O	1:7	0.22	0.20
MON1 + H ₂ O	1:12	0.12	0.11
MON1 + H ₂ O	1:20	0.11	0.11

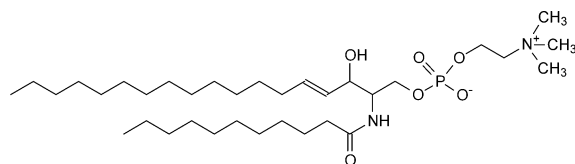
dramatically, indicating the formation of oligomers of MON1 with higher molecular weights, by a self-assembling process. Addition of more water molecules (stoichiometry 1:12) still leads to a slight decrease in the osmotic coefficient, showing that the self-assembly process still progresses, leading to the formation of oligomers of even higher stoichiometry, such as 8–9 MON1 units. In contrast, the use of MON1/water at ratios higher than 1:12 has no influence on the value of the osmotic coefficient, which means that under the experimental conditions the formation of a chain made up of at most ten MON1 units is feasible. These results are in line with the fact that the intensity of the continuous absorption as a marker for the chain length in which the proton can move does not further increase with MON1/water stoichiometries higher than 1:12.

PM5 Calculations. The values for the heat of formation (HOF) of water-free MON1 and its complexed and uncomplexed species are given in Table 3. The index “uncomplexed” indicates the sum of the heats of formation for separated MON1 and water molecules assuming that there is no interaction between them. The index “complexed” refers to the HOF values obtained taking into account the interactions between the molecules. The values are given for the complexes of monensin with various numbers of water molecules in the gas phase and for the species based on the (MON1 + 3H₂O) unit formed by the self-assembly process in the gas phase and in the lipid bilayer. From these two HOF values, the Δ HOF values were calculated. The Δ HOF values reflect the energetic profit of the complexation process between water and monensin and the energetic profit of the self-assembly process of the (MON1 + 3H₂O) unit, respectively. Table 3 gives the energetic profit calculated per one water molecule (Δ HOF/(H₂O)_x, x = number of water molecules) and per one (MON1 + 3H₂O) species (Δ HOF/(MON1 + 3H₂O)_n, n = number of (MON1 + 3H₂O) species). With increasing

TABLE 3: Heats of Formation (kcal/mol) of MON1 and Its Hydrates Calculated in the Gas Phase and in the Lipid Bilayer by the PM5 Method (WinMopac 2003)^a

hydrates	HOF (kcal/mol)	Δ HOF (kcal/mol)	Δ HOF/(H ₂ O) _x (kcal/mol)	Δ HOF/(MON1 + 3H ₂ O) _n (kcal/mol)
in the gas phase				
MON1	-538.81			
MON1 + H ₂ O uncomplexed	-592.50	-21.61	-21.61	
MON1 + H ₂ O complexed	-614.11			
MON1 + 2H ₂ O uncomplexed	-647.30	-57.44	-28.72	
MON1 + 2H ₂ O complexed	-704.74			
MON1 + 3H ₂ O uncomplexed	-701.20	-91.48	-30.49	-91.48
MON1 + 3H ₂ O complexed	-792.68			
MON1 + 4H ₂ O uncomplexed	-755.10	-108.44	-27.11	
MON1 + 4H ₂ O complexed	-863.54			
(MON1 + 3H ₂ O) ₂ uncomplexed	-1410.49	-223.41	-37.24	-111.71
(MON1 + 3H ₂ O) ₂ complexed	-1633.90			
(MON1 + 3H ₂ O) ₄ uncomplexed	-2831.17	-515.13	-42.93	-128.78
(MON1 + 3H ₂ O) ₄ complexed	-3346.30			
(MON1 + 3H ₂ O) ₈ uncomplexed	-5687.34	-1061.28	-44.21	-132.66
(MON1 + 3H ₂ O) ₈ complexed	-6748.62			
in the lipid bilayer (sphingolipids)				
	^b			
(MON1 + 3H ₂ O) ₈ uncomplexed	-5723.92	-1084.59	-45.19	-135.57
(MON1 + 3H ₂ O) ₈ complexed	-6808.51			
(MON1 + 3H ₂ O) ₉ uncomplexed	-6434.45	-1095.12	-40.56	-121.68
(MON1 + 3H ₂ O) ₉ complexed	-7529.57			
(MON1 + 3H ₂ O) ₁₀ uncomplexed	-7145.40	-1101.64	-36.72	-110.16
(MON1 + 3H ₂ O) ₁₀ complexed	-8247.04			

^a x and n represent numbers. ^b $\text{HOF}_{\text{total}} - \text{HOF}_{\text{lipid bilayer}}$

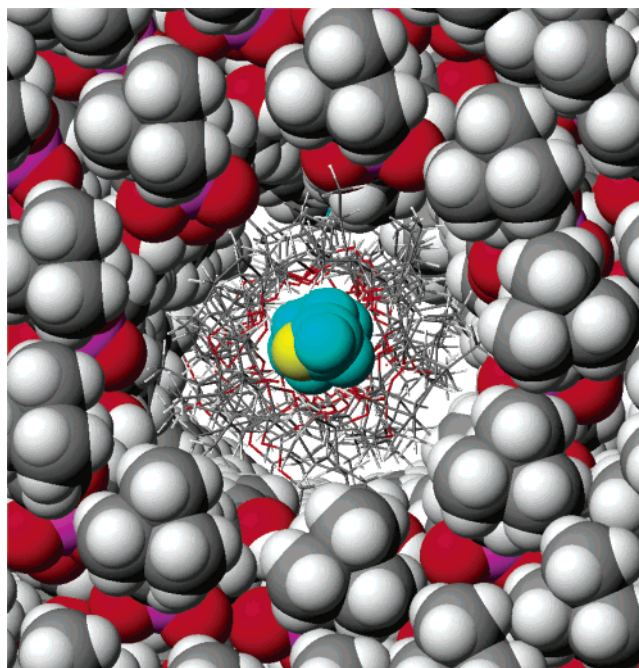
CHART 5: Sphingomyelin: The Basic Unit of the Membrane Model Used in the PM5 Calculations

numbers of water molecules, up to three molecules bonded with a monomeric MON1 molecule, these values decrease. With the addition of a fourth water molecule, the Δ HOF value slightly decreases, whereas the Δ HOF/(H₂O)_x value increases. This result demonstrates that the fourth water molecule does not fit into the structure of MON1 with three water molecules, i.e., (MON1 + 3H₂O) species, which seems to be more favorable than the monomeric one.

Most striking are the results of the energetic profits of the self-assembly process of the (MON1 + 3H₂O) species. With progressive formation of the proton channel, the calculated values of the energetic profits for Δ HOF/(H₂O)_x and for $[\Delta$ HOF/(MON1 + 3H₂O)_n] strongly decrease. This shows that the formation of the hydrophobic monensin part of the channel and the formation of a chain of water molecules in the inner core are both energetically favorable, increasing the probability of formation of a proton-conducting channel.

The semiempirical calculations suggest that the formation of a proton channel in the lipid bilayer (Charts 6 and 7), built on sphingomyelin (Chart 5), by a self-assembly process of the (MON1 + 3H₂O)_n species is energetically most favorable in the case of $n = 8$. The association of the ninth and tenth (MON1 + 3H₂O) species does not contribute to the stability of the channel as shown by the fact that the values for the heat of formation decrease for $n = 9$ and 10 (Table 3).

Table 4 presents the lengths and angles of the hydrogen bonds formed within the MON1 molecule and in the (MON1 + 3H₂O) species as well as the hydrogen bonds involved in the self-assembly process. These values suggest that all hydrogen bonds stabilizing the calculated structure are rather weak as indicated

CHART 6: View down the Axis of the Hypothetical Proton Channel Structure Made Up of Eight (MON1 + 3H₂O) Species, Calculated by the PM5 Method in the Lipid Bilayer Containing Sphingolipids

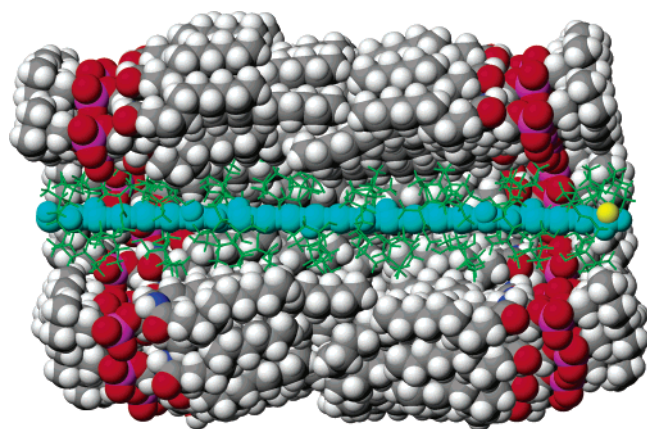
by their bond angles strongly deviating from the angle of 180° observed for strong hydrogen bonds.

The (MON1 + 3H₂O) monomers forming the (MON1 + 3H₂O)₈ octameric structure are bonded via hydrogen bonds to each other alternately in the head–head and tail–tail configuration. The structures of the MON1 and (MON1 + 3H₂O) species and of the proton channel (MON1+3H₂O)₈ are shown in Charts 2–4. MON1 forms a pseudo-ring structure mainly stabilized by three intramolecular hydrogen bonds. The structure of MON1, involving three water molecules, also has a pseudo-ring character in which the water molecules are bonded to

TABLE 4: Lengths (Å) and Angles (deg) of the Hydrogen Bonds in MON1 and Its Hydrates Calculated by the PM5 Method (WinMopac 2003)^a

compound	O atom	hydrogen bond length (Å)				hydrogen bond angle (deg)			
		O _{IV} H	O _X H	O _{XI} H	HO _{H2O}	O _{IV} H	O _X H	O _{XI} H	HO _{H2O}
MON1	O _{II}		2.91	2.97			132.3	131.8	
MON1 + 3H ₂ O	O _{IX}	2.67				151.0			
	O _{VIII}				2.56				109.0
	O _{IV} ⁻				2.63				136.3
	O _{IX}				2.47				106.7
	O _{H2O}		2.81	2.81	2.59		120.1	119.9	153.5
	O _{VII}				2.63				121.1
	O _{II}			2.98				130.8	
	O _{VI}				2.55				116.3
	O _V				2.91				174.1
	O _{III}				2.51				114.9
Hydrogen Bonds Joining the (MON1 + 3H ₂ O) Species in Octameric Structure									
A–B	O _{II} (A)			2.59				112.6	
	O _{II} (B)			2.64				113.2	
B–C	O _{VIII} (C)	2.68				134.9			
	O _{IX} (B)	2.68				123.5			
C–D	O _{II} (D)			2.75				116.2	
	O _{II} (C)			2.70				117.1	
D–E	O _{VIII} (E)		2.92				147.6		
	O _{VIII} (D)	2.88				143.5			
E–F	O _{II} (F)			2.57				110.1	
	O _{II} (E)			2.58				109.4	
F–G	O _{VIII} (G)	2.63				131.7			
	O _{VIII} (F)	2.72				126.1			
G–H	O _{II} (H)			2.71				113.4	
	O _{II} (G)			2.81				157.2	

^a A, B, C, D, E, F, G, and H are the respective (MON1 + 3H₂O) species.

CHART 7: View of the Hypothetical Proton Channel Made Up of Eight (MON1 + 3H₂O) Species along Its Axis Calculated by the PM5 Method in the Lipid Bilayer Containing Sphingolipids

various proton donor and proton acceptor groups and are almost linear to each other. In this structure, the initial proton (marked by yellow, Chart 3) is located at the entrance of the channel formed by the pseudo-ring units, but due to its large polarizability, it can fluctuate very quickly between all water molecules as indicated by the continuous absorption discussed above. The association of the eight (MON1 + 3H₂O) units leads to the formation of a channel, whose length of about 60 Å is comparable to the thickness of a lipid bilayer. The proton channel is formed by 24 almost linear hydrogen-bonded water molecules (in the gas phase (Chart 4) and in the lipid bilayer along the proton channel axis (Chart 7)). The stereochemical view down the proton channel axis is shown in Chart 6. Rough estimated diameters of the channels in the gas phase and in the lipid bilayer are 5.0 and 4.5 Å, respectively.

Conclusions

In the present study, we show that the methyl ester of monensin A (MON1) is able to form hydrates with up to three water molecules hydrogen-bonded inside a pseudo-ring structure. This ability of MON1 is made possible by the transfer of a proton from the O_{IV}–H hydroxyl group to an oxygen atom of a water molecule. In this way, the water molecule becomes protonated and solvated by one or two additional water molecules. In the solvated structure, the water molecules form an almost linear hydrogen-bonded chain in which the excess proton can fluctuate as indicated by a continuous absorption in the FTIR spectra. The presence of the (MON1 + 3H₂O) species as pseudo-ring structures leads to a self-assembly process with the formation of a proton channel in which the initial proton can move within the whole channel, indicated by the increasing intensity of the continuous absorption.

Semiempirical calculations suggest that in the lipid bilayer such a proton channel can possibly consist of eight pseudo-ring (MON1 + 3H₂O) species. Thus, we suggest for the first time, the possibility that a modified ionophore can transport protons across the cell lipid bilayer via the formation of a proton channel instead of forming defined complexes with the proton and moving through the bilayer, which is how transport is thought of classically.

Acknowledgment. P.P. thanks the Foundation of Polish Science for a fellowship.

References and Notes

- (1) Agtarap, A.; Chamberlin, J. W.; Pinkerton, M.; Steinrauf, I. *J. Am. Chem. Soc.* **1967**, *89*, 5737.
- (2) Honey, M. E.; Hoehn, M. M. *Antimicrob. Agents Chemother.* **1967**, *349*.
- (3) Riddell, F. G. *Chirality* **2002**, *14*, 121.
- (4) Duax, W. L.; Smith, G. D.; Strong, P. D. *J. Am. Chem. Soc.* **1980**, *102*, 6725.

- (5) Ward, D. L.; Wei K. T.; Hoogerheide, J. C.; Popov, A. I. *Acta Crystallogr., Sect. B* **1978**, *34*, 110.
- (6) Pinkerton, M.; Steinrauf, L. K. *J. Mol. Biol.* **1970**, *49*, 533.
- (7) Pangborn, W.; Duax, W.; Langa, D. *J. Am. Chem. Soc.* **1987**, *109*, 2163.
- (8) Martinek, T.; Riddell, F. G.; Wilson, C.; Weller, C. T. *J. Chem. Soc., Perkin Trans. 2* **2000**, 35.
- (9) Dauphin, G.; Jeminet, G.; Vaufray, F. *J. Chem. Soc., Perkin Trans. 2*, **1993**, 399.
- (10) Ferdani, R.; Gokel, G. W. Ionophores. In *Encyclopedia of Supramolecular Chemistry*; Atwood, J. L., Steed, J. W., Eds.; Marcel Dekker: New York, 2004; p 760.
- (11) In *Polyether Antibiotics: Naturally Occurring Acid Ionophores*; Westley, J. W., Ed.; Marcel Dekker: New York, 1982; Vol. 1, p 1.
- (12) In *Polyether Antibiotics: Naturally Occurring Acid Ionophores*; Westley, J. W., Ed.; Marcel Dekker: New York, 1983; Vol. 2, p 51.
- (13) Pressman B. C. In *Antibiotics and Their Complexes*; Sigel, H., Sigel, A., Eds.; Marcel Dekker: New York, 1985; p 1.
- (14) Sandeaux, R.; Sandeaux, J.; Gavach, C.; Brun, B. *Biochim. Biophys. Acta* **1982**, *68*, 127.
- (15) Nakazato, K.; Hanato, Y. *Biochim. Biophys. Acta* **1991**, *1064*, 103.
- (16) Riddell, F. G.; Arumugam, S.; Cox, B. G. *Biochim. Biophys. Acta* **1988**, *944*, 279.
- (17) Antonenko, Y. N.; Yagushinsky, L. S. *Biochim. Biophys. Acta* **1988**, *938*, 125.
- (18) Gaboyard, C.; Dauphin, G.; Vaufray, F.; Jeminet, G. *Agric. Biol. Chem.* **1990**, *54*, 1149.
- (19) Ben-Tal, N.; Sitko, D.; Bransburg-Zabary, S.; Nachliel, E.; Gutman, M. *Biochim. Biophys. Acta* **2000**, *1466*, 221.
- (20) Hebrant, M.; Pointud, Y.; Juillard, J. *J. Phys. Chem.* **1991**, *95*, 3653.
- (21) Pressman, B. C. *Annu. Rev. Biochem.* **1976**, *45*, 501.
- (22) Pressman, B. C.; Fahim, M. *Annu. Rev. Pharmacol. Toxicol.* **1982**, *22*.
- (23) Liu, C. In *Polyether Antibiotics: Naturally Occurring Acid Ionophores*; Westley, J. W., Ed.; Marcel Dekker: New York, 1982; Vol. 1, p 43.
- (24) Russell, J. B. *J. Anim. Sci.* **1987**, *64*, 1519.
- (25) Edrington, T. S.; Callaway, T. R.; Varey, P. D.; Jung, Y. S.; Bischoff, K. M.; Elder, R.; Anderson, R. C.; Kutter, E.; Brabban, A. D.; Nisbet, D. J. *J. Appl. Microbiol.* **2003**, *94*, 207.
- (26) Reid, W. M.; Kowalski, L.; Rice, J. *Poult. Sci.* **1972**, *51*, 46.
- (27) Dennis, S. M.; Nagaraja, T. G.; Bartley, E. E. *J. Anim. Sci.* **1981**, *52*, 418.
- (28) Ruff, M. D. In *Polyether Antibiotics: Naturally Occurring Acid Ionophores*; Westley, J. W., Ed.; Marcel Dekker: New York, 1982; Vol. 1, p 304.
- (29) Stephen, B.; Rommel, M.; Dauschies, A.; Haberkorn, A. *Vet. Parasitol.* **1997**, *69*, 19.
- (30) Osborne, M. W.; Wenger, J.; Kovzelove, F.; Boyd, R.; Zanko, M. In *Polyether Antibiotics: Naturally Occurring Acid Ionophores*; Westley, J. W., Ed.; Marcel Dekker: New York, 1982; Vol. 1, p 333.
- (31) McGuffey, R. K.; Richardson, L. F.; Wilkinson, J. I. D. *J. Dairy Sci.* **2001**, *84E*, 194.
- (32) Haimoud, D. A.; Bayourthe, C.; Moncoulon, R.; Verney, M. *J. Sci. Food Agric.* **1996**, *70*, 181.
- (33) Ipharraguerre, I. R.; Clark, J. H. *Anim. Feed. Sci. Technol.* **2003**, *106*, 39.
- (34) Ramanzin, M.; Bailoni, L.; Schiavon, S.; Bittante, G. *J. Dairy Sci.* **1997**, *80*, 1136.
- (35) Frigg, M.; Broz, J.; Weber, G. *Arch. Geflügelkd.* **1983**, *47*, 20.
- (36) Bergen, W. G.; Bates, D. B. *J. Anim. Sci.* **1984**, *58*, 83.
- (37) Langson, V. C.; Galey, F.; Lowell, R.; Buc, W. B. *Vet. Med.* **1985**, *8075*.
- (38) Johnson, D. C.; Schlessinger M. *J. Virol.* **1980**, *103*, 407.
- (39) Schlegel, R.; Willingham, M.; Pastan, I. *Biochem. Biophys. Res. Commun.* **1981**, *102*, 992.
- (40) Marsh, M.; Wellstead, J.; Kern, H.; Harms, E.; Helenius, A. *Proc. Natl. Acad. Sci. U.S.A.* **1982**, *79*, 5297.
- (41) Iacoangeli A.; Melucci-Vigo, G.; Risuleo, G. *Biochimie* **2000**, *82*, 35.
- (42) Tanabe, K. *Blood Cells* **1990**, *16*, 437.
- (43) Adovelande, J.; Schrevel, J. *Life Sci.* **1996**, *59*, 309.
- (44) Nagatsu, A.; Tanaka, R.; Hashimoto, M.; Mizukami, H.; Ogihara, Y.; Sakakibara, J. *Tetrahedron Lett.* **2000**, *41*, 2629.
- (45) Tanaka, R.; Nagatsu, A.; Mizukami, H.; Ogihara, Y.; Sakakibara, J. *Tetrahedron* **2001**, *57*, 3005.
- (46) Nagatsu, A.; Takahashi, T.; Isomura, M.; Nagai, S.; Ueda, T.; Murakami, N.; Sakakibara, J.; Hatano, K. *Chem. Pharm. Bull.* **1994**, *42*, 2269.
- (47) Sakakibara, J.; Nakamura, A.; Nagai, S.; Ueda, T.; Ishida, T. *Chem. Pharm. Bull.* **1988**, *36*, 4776.
- (48) Tanaka, R.; Nagatsu, A.; Mizukami, H.; Ogihara, Y.; Sakakibara, J. *Chem. Pharm. Bull.* **2001**, *49*, 711.
- (49) Tsukube, H.; Sohmiya, H. *J. Org. Chem.* **1991**, *56*, 875.
- (50) Maruyama, K.; Sohmiya, H.; Tsukube, H. *Tetrahedron* **1992**, *48*, 805.
- (51) Nagatsu, A.; Tabunoki, Y.; Nagai, S.; Ueda, T.; Sakakibara, J.; Hidaka, H.; *Chem. Pharm. Bull.* **1997**, *45*, 966.
- (52) Sedmera, P.; Pospisil, S. *Collect. Czech. Chem. Commun.* **1997**, *64*, 7703.
- (53) Tohda, K.; Suzuki, K.; Kosuge, N.; Watanabe, K.; Nagashima, H.; Inoue, H.; Shirai, T. *Anal. Chem.* **1990**, *62*, 936.
- (54) Huczyński, A.; Przybylski, P.; Brzezinski, B.; Bartl, F. *Biopolymers* **2006**, *81*, 282.
- (55) Stewart, J. J. P. *J. Comput. Chem.* **1989**, *10*, 209.
- (56) Stewart, J. J. P. *J. Comput. Chem.* **1991**, *12*, 320.
- (57) *CAChe 5.04 UserGuide*; Fujitsu: Chiba, Japan, 2003.
- (58) Walrafen, G. E. *J. Chem. Phys.* **1966**, *44*, 1546.
- (59) Taylor, M. J.; Walley, E. *J. Chem. Phys.* **1964**, *40*, 1660.
- (60) Zundel, G. In *Electron and Proton Transfer in Chemistry and Biology*; Mueller, A., Ratajczak-Junge, H., Diemann, W., Eds.; Elsevier: Amsterdam, 1992; p 313.
- (61) Brzezinski, B.; Bartl, F.; Zundel, G. *J. Phys. Chem. B* **1997**, *101*, 5607.
- (62) Eckert, M.; Zundel, G. *J. Phys. Chem.* **1988**, *92*, 7016.
- (63) Nakazato, K.; Hatano, Y. *Biochim. Biophys. Acta* **1991**, *1064*, 103.
- (64) Zhu, W.-H.; Loh, T.-T. *Biochim. Biophys. Acta* **1995**, *1269*, 122.
- (65) Mollenhauer, H. H.; Morre, D. J.; Rowe, L. D. *Biochim. Biophys. Acta* **1990**, *1031*, 225.
- (66) Nachliel, E.; Finkelstein, Y.; Gutman, M. *Biochim. Biophys. Acta* **1996**, *1285*, 131.
- (67) Bartl, F.; Brzezinski, B.; Różalski, B.; Zundel, G. *J. Phys. Chem.* **1998**, *102*, 5234.
- (68) Garczarek, F.; Brown, L. S.; Lanyi, J. K.; Gerwert, K. *Proc. Natl. Acad. Sci. U.S.A.* **2005**, *102*, 3633.